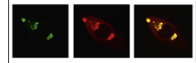


Available online at www.sciencedirect.com

ScienceDirect

www.elsevier.com/locate/brainres

Brain Research



Research Report

C57BL/6J congenic Prp-TDP43A315T mice develop progressive neurodegeneration in the myenteric plexus of the colon without exhibiting key features of ALS

Theo Hatzipetros^{a,1}, Laurent P. Bogdanik^{b,1}, Valerie R. Tassinari^a,
 Joshua D. Kidd^a, Andy J. Moreno^a, Crystal Davis^b, Melissa Osborne^b,
 Andrew Austin^b, Fernando G. Vieira^{a,*}, Cathleen Lutz^{b,**}, Steve Perrin^a

^aALS Therapy Development Institute, 300 Technology Square, Suite 400, Cambridge, MA 02139, USA

^bThe Jackson Laboratory, 600 Main Street, Bar Harbor, ME 04609, USA

ARTICLE INFO

Article history:

Accepted 8 October 2013

Keywords:

ALS

TDP-43

RNA binding

Transgenic animal models

Proteinopathy

Prion

Neurodegeneration

Myenteric plexus

ABSTRACT

ALS therapy development has been hindered by the lack of rodent animal models. The discovery of TDP-43, a transcription factor that accumulates in the cytoplasm of motor neurons (MNs) in most cases of ALS, prompted attempts to develop TDP-43-based models of the disease. The current study sought to examine, in extensive detail, the emerging disease phenotype of a transgenic mouse model that overexpresses a mutant human TDP-43 (hTDP-43) gene under mouse prion promoter control. Careful attention was given to ALS-like characteristics to determine the appropriateness of this model for testing therapies for ALS. In light of previous reports that gastrointestinal (GI) dysfunction is responsible for early death in these mice, gut immunohistochemistry (IHC) and longitudinal gut motility assays were used to identify the onset and the progression of these defects. IHC studies revealed that site-specific overexpression of the hTDP-43 transgene in colonic myenteric plexes resulted in progressive neurodegeneration in this region. This change was associated with progressively reduced GI motility, culminating in frank stasis that was primarily responsible for decreasing longevity in these mice. The disease phenotype was gender- and genetic background-dependent, with congenic C57BL/6J male mice exhibiting the most aggressive form of the disease. Spinal cord IHC revealed ubiquitin-positive inclusions, but not TDP-43 aggregates, in the cytoplasm of MNs. Neither gender exhibited compelling ALS-like neuromuscular deficits, irrespective of age. While this model may be useful for studying GI tract neurodegeneration, in its present state it does not display a phenotype suitable for testing ALS therapeutics.

This article is part of a Special Issue entitled RNA Metabolism 2013.

© 2013 Elsevier B.V. All rights reserved.

*Corresponding author. Fax: +1 617 441 7299.

**Corresponding author.

E-mail addresses: fvieira@als.net (F.G. Vieira), Cat.Lutz@jax.org (C. Lutz).

¹These authors contributed equally to the publication.

1. Introduction

Amiotrophic lateral sclerosis (ALS) is an adult-onset neurological disorder characterized by the loss of upper and lower motor neurons (MNs), degeneration of the corticospinal tracts and reactive gliosis in the brains and spinal cords of patients (Ghatak et al., 1986; Schiffer et al., 1996; Murayama et al., 1991). Clinical manifestations of these pathologies include progressive weakness, muscular atrophy with eventual paralysis, and death (Rowland and Shneider, 2001). Another disease hallmark is the occurrence of ubiquitin-positive cytoplasmic inclusions in degenerating motor neurons and surrounding astrocytes (Leigh et al., 1991; Barbeito et al., 2004), however the contribution of these inclusions to the overall course of the disease remains unclear. The majority of ALS cases (90–95%) are of unknown etiology and are considered sporadic ALS (SALS), while the remaining 5–10% of ALS cases are genetic or familial (FALS) with a predominantly Mendelian pattern of inheritance (Swarup and Julien, 2011). There is currently no cure for ALS and death usually occurs within five years from the onset of symptoms.

The development of treatments for ALS has been hindered by a shortage of preclinical tools (animal models, cellular assays, biomarkers, etc.). The first mouse model of the disease was developed in the mid 1990s (Gurney et al., 1994) following the identification of mutations in the copper/zinc superoxide dismutase 1 (SOD1) gene linked to 20% of FALS cases (Rosen et al., 1993). This widely used mouse model, genetically engineered to overexpress a mutant form of the human SOD1 gene harboring the ALS-associated glycine to alanine mutation at amino acid 93 (SOD1 G93A), recapitulated many of the pathological features of ALS in humans (MN loss, progressive muscle weakness, paralysis, and decreased survival) and it promised to become an important *in vivo* screening tool for ALS therapies. Unfortunately, with the exception of riluzole (Gurney et al., 1996), no effective therapy for ALS patients has been identified to date in the SOD1 mouse (Gordon and Meininger, 2011). The failure to translate positive preclinical results from the SOD1 mouse model into clinical efficacy has raised questions about the optimal design of preclinical studies (Scott et al., 2008; Ludolph et al., 2010) and clinical trials (Aggarwal and Cudkovic, 2008). More importantly, the suitability of the transgenic SOD1 mouse as a standalone model of non SOD1-linked FALS and SALS was called into question (Benatar, 2007).

More recent discoveries have implicated the gene encoding the transactive response DNA-binding protein 43 (TDP-43), a protein involved in DNA/RNA processing, with the etiology of both SALS and FALS. This has led to the development of new and potentially impactful TDP-43-based animal models of ALS. Aberrant TDP-43 protein function was directly linked with the neurodegeneration in ALS by two key pieces of evidence. Initially, TDP-43 was recognized as the main component of the ubiquitin-positive cytoplasmic inclusions present in the majority of SALS patients (Neumann et al., 2006; Arai et al., 2006), and later missense mutations in the TDP-43 gene were identified in patients with FALS (Sreedharan et al., 2008; Gitcho et al., 2008). The first TDP-43 transgenic mouse model was developed by overexpressing the mutant human

TDP-43 gene, harboring the alanine to threonine mutation at amino acid 315, under the control of the mouse prion promoter (Prp-TDP43A315T; Wegorzewska et al., 2009). Prp-TDP43A315T mice reportedly developed a progressive and fatal neurodegenerative disease with pathology reminiscent of ALS. Additionally, several important features of the human disease were apparently replicated in these mice. These included gait abnormalities, selective vulnerability of cortical and spinal MNs, and ubiquitin aggregate pathology albeit without the presence of cytoplasmic TDP-43 aggregates (Wegorzewska et al., 2009) that occurs in humans. This original phenotypic assessment was performed on a mixed C57BL/6 and CBA genetic background. Two subsequent studies however reported that the cause of death in the Prp-TDP43A315T mice on a pure C57BL/6J genetic background was not related to the MN loss, but was instead due to gastrointestinal (GI) dysfunction (Esmaili et al., 2013; Guo et al., 2012). However, conclusions from these two studies relied heavily on gross anatomical and histological experiments performed on GI tract tissue from deceased or moribund Prp-TDP43A315T mice. The onset and the etiology of this pathology were not thoroughly investigated and the possibility that GI dysfunction could have been the consequence of a neurodegenerative process was not discussed. Thus, it remains unclear whether the Prp-TDP43A315T mouse model in its present genetic state can serve as a valid, new animal model of ALS and more research is required to answer this question.

The overall objective of this study was to examine the emerging phenotype in the Prp-TDP43A315T mouse model (JAX stock 10700, B6.Cg-Tg(Prnp-TARDBP^{A315T})95Balo/J) and determine whether aspects of this phenotype could be used for testing therapeutic strategies for ALS. For drug development purposes, these transgenic animals should ideally recapitulate key features of ALS including MN loss, progressive muscular weakness, motor deficits, and decreased survival. Additionally, early disease onset, slow progression and low variability are very desirable. To accomplish this objective, over 650, transgenic male and female C57BL/6J congenic Prp-TDP43A315T mice were bred and phenotypically characterized. In light of the evidence showing that GI dysfunction might be responsible for the death of these mice, longitudinal gut motility assays were also used to identify the onset and the progression of this pathology. Neuromotor performance was examined as a function of age. Muscle strength was evaluated using the grip strength method and the hanging wire test. Finally, immunohistochemical techniques were utilized to assess neuropathology in the spinal cord and the gut.

2. Results

2.1. Body weights and survival of Prp-TDP43A315T mice

At birth and during the first weeks of development, C57BL/6J congenic Prp-TDP43A315T (TDP-43) mice of both genders appeared normal and weighed the same as their wild-type (WT) littermates (Fig. 1). On average, male TDP-43 mice reached their maximum weight of 31.8 ± 0.4 g at post-natal day 81. At that time, the weight of age-matched, male, non-transgenic littermates was not significantly different at

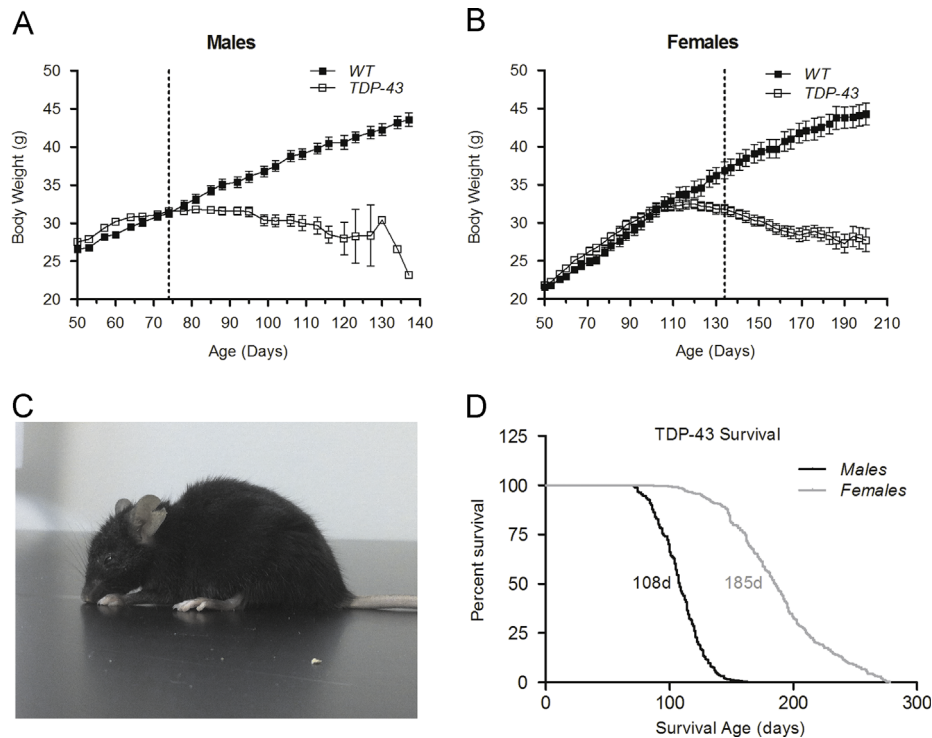


Fig. 1 – Body weights and survival curves. Body weights of male (A; $n=60$ TDP-43, 29 WT) and female (B; $n=56$ TDP-43, 30 WT) mice. The dotted vertical lines represent the time of the first mouse death in the respective cohort. Photograph of a representative moribund TDP-43 male mouse (C). Kaplan–Meier curve showing the survival of male and female TDP-43 mice (D; $n=315$ male, 305 female). Body weight values represent the mean \pm SEM.

33.2 ± 0.6 g (Fig. 1A). On average, female TDP-43 mice reached their maximum weight of 32.5 ± 0.7 g at post-natal day 110. At the same time the weight of age-matched, female, non-transgenic littermates was not significantly different at 33.7 ± 1.1 g (Fig. 1B). There was a statistically significant weight loss occurring after post-natal day 85 in males and after post-natal day 127 in females. This weight loss coincided with a decline in overall health characterized by immobility, kyphosis, an unkempt haircoat, dehydration, swollen and tender abdomen, and difficulty righting (Fig. 1C). The onset of the disease was sudden and the progression was rapid, especially in the case of males. In males, death usually occurred within 2 weeks of onset and within 4 weeks in females. The median life expectancies of TDP-43 transgenic mice were 108 days for the males and 185 days for the females (Fig. 1D).

2.2. Prp-TDP43A315T mice exhibited severe gastrointestinal pathology

To gain insights on the cause of early death, autopsies were performed on randomly selected male and female TDP-43 mice. There was noticeable pathology detected in the lower GI tract, distal to the cecum, comprised of swelling, intra-intestinal coagulated blood and necrotic tissue. In contrast, gross examination of the upper digestive tract and other internal organs did not reveal any obvious gross pathology. Further, no pathology was detected in age-matched, euthanized WT mice. Since pathology within the GI tract has a direct impact on the rate of gastric emptying, gut motility, and transit time (Knowles and Martin, 2000), an assay was

implemented to measure the gut motility of TDP-43 mice as means of assessing the onset and progression of GI pathology (Section 4). It was hypothesized that intestinal transit times would increase (slower gut motility) proportionately to the severity of GI pathology. The assay was performed for the first time when the mice were 50 days old, and at that time there were no identified signs of GI pathology. The intestinal transit times of TDP-43 male and female mice were 4.1 ± 0.1 and 4.0 ± 0.2 h respectively, and they were not significantly different from the intestinal transit times of age and gender matched WT controls (Fig. 2). By post-natal day 60, the average intestinal transit time of male TDP-43 mice had dramatically increased to 6.6 ± 0.2 h (Fig. 2A) or 183% of WT controls (Fig. 2C). This suggested that there was a change in GI function or health between days 50 and 60. In contrast, at 60 days the intestinal transit time of female mice was not significantly different from that of WT controls (Fig. 2B). The intestinal transit time of male TDP-43 mice progressively increased with age and by post-natal age day 90 it was 11.5 ± 0.8 h or 282% of WT controls. The intestinal transit time of female TDP-43 mice also increased with age and was also significantly different compared to WT mice, however this change happened later in life and was not as severe as in the males. Consistent with the slowing down of gut motility, the number of fecal pellets excreted by TDP-43 mice progressively decreased and close to the end of their lives hardly any fecal pellets were excreted (data not shown). It is interesting to note that male and female SOD1G93A transgenic mice, the most widely used animal model of ALS, did not show significant deficits in the same gut motility assay (Fig. S1).

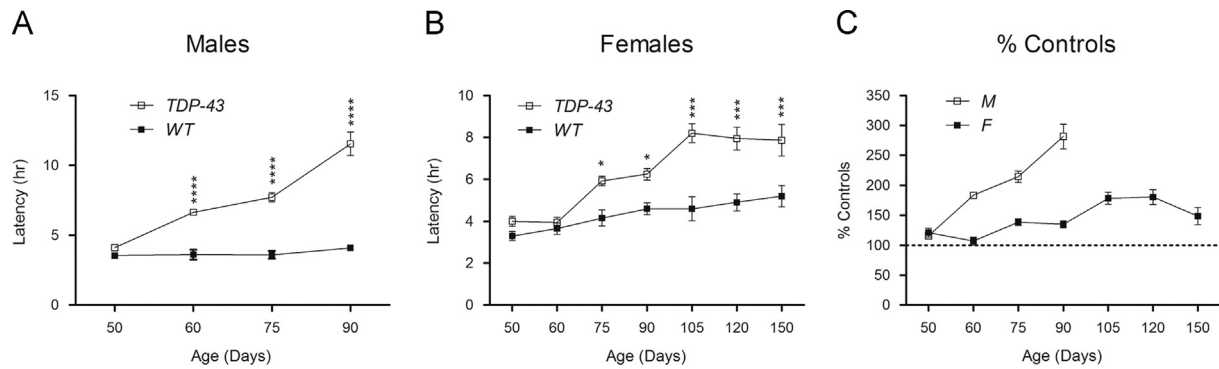


Fig. 2 – Gut motility assay. Intestinal transit time was assessed by time in hours required for the appearance of the first blue pellet after the administration of 0.3 ml of blue dye via oral gavage in male (A; $n=39$ TDP-43, 21 WT) and female (B; $n=37$ TDP-43, 20 WT) mice. The % change in intestinal transit time between TDP-43 and WT mice (C). Values represent the mean \pm SEM.

2.3. Transgene overexpression in the colon led to neurodegeneration

To determine whether the observed pathology in the lower GI tract was related to the degree of hTDP-43 transgene expression in this region, immunofluorescence using an anti-Flag antibody was performed on myenteric plexus tissue derived from the *duodenum* (proximal to the cecum) and the *colon* (distal to the cecum) of 80 day old, male TDP-43 mice with clear signs of GI dysfunction. The myenteric (Auerbach's) plexus is a network of nerve fibers arising from the vagus nerve that innervate the muscular lining of the GI tract. It is primarily responsible for the neural control of gut motility (Marieb and Hoehn, 2012). Results from this experiment indicated that the hTDP-43 transgene was broadly expressed in neurons of the myenteric plexus derived from the *colon* (Fig. 3B), but only in very few neurons of the myenteric plexus derived from the *duodenum* (Fig. 3A).

The myenteric plexus was stained for acetylcholinesterase (AChE) activity. This technique was previously demonstrated to be effective in labeling the nerve fibers and pericaryons of the myenteric plexus which are mostly cholinergic (Maiffrino et al., 1999). There was no difference in the AChE staining of myenteric plexus from the *duodenum* between TDP-43 (Fig. 3C) and WT mice (Fig. 3D). However, AChE staining of myenteric plexus from the *colon* showed significantly decreased staining in the ganglions and internodal strands of TDP-43 mice (Fig. 3F), compared to WT mice (Fig. 3E). This suggests that there were decreased numbers of cholinergic neurons. AChE staining also revealed decreased ganglionic cellularity in TDP-43 mice compared to WT mice (Fig. 3E and F, insets).

To examine whether the hTDP-43 transgene overexpression in the myenteric plexus of the *colon* resulted in neuronal loss in this region, the entire neuronal population was labeled using the neuron-specific marker cuproline blue (Van Ginneken et al., 1999). Cuproline blue staining of the ganglion neurons in the myenteric plexus of the *colon* revealed a massive neuronal loss in the TDP-43 mice (Fig. 3H), that amounted to an 80% loss of cells compared to the WT mice (Fig. 3G). This severe neuronal loss was only observed in the *colon* of older (90–150 day old) TDP-43 mice. A milder, non-significant, neuronal loss was observed in the *colon* of

younger (30–60 day old) TDP-43 mice (Fig. 3J). No neuronal loss was observed in the *duodenum* (Fig. 3I). Together, these results showed that hTDP-43 transgene overexpression in the lower GI tract of TDP-43 mice resulted in progressive neurodegeneration.

GI motility is also partially regulated by the sympathetic nervous system and for this reason hTDP-43 transgene expression was also assessed in the superior mesenteric ganglion (SMG) using anti-Flag immunofluorescence (Supplemental Materials). The results showed that the transgene was highly expressed in the nuclei of SMG neurons (Fig. S3 A and B). Additionally, the ganglions of TDP-43 mice appeared smaller when compared to those of WT mice, and they had an increased percentage of condensed nuclei (Fig. S3C–E) indicating TDP-43 transgene-dependent changes in the SMG.

2.4. Prp-TDP43A315T mice showed minimal neuromuscular deficits

Starting at 50 days of age, mice were evaluated twice a week using a modified version of the SHIRPA protocol that concentrated on identifying neurological abnormalities (Section 4). Collectively, the results from these evaluations showed that TDP-43 mice were phenotypically very similar to their WT littermates. Specifically, they appeared to have a normal body position, no limb clasping, no signs of paralysis, no trunk curling, no tremor, nor any other identifiable abnormality (data not shown). Further, there were no abnormalities in gait stride length or stance width using the footprint test, at any of the times tested (Fig. S2). Finally, tests used to assess neurological reflexes showed that TDP-43 mice had generally comparable *forelimb* and *hindlimb* reflexes with their WT littermates (Fig. 4A and B). Mild deficits in the *hindlimb* reflex of moribund male and female TDP-43 mice were present (Fig. 4B), but there were never any signs of significant limb weakness or paresis (score 3 or higher). It is noteworthy that the onset of GI pathology did not have a substantial impact on neurological reflexes (Fig. 4A and B, shaded areas).

There was one notable exception in the comparability of WT and TDP-43 SHIRPA evaluation results. This exception involved a deficit in the tail position of TDP-43 mice (Fig. 4C). TDP-43 mice of both genders had the tendency to drag their

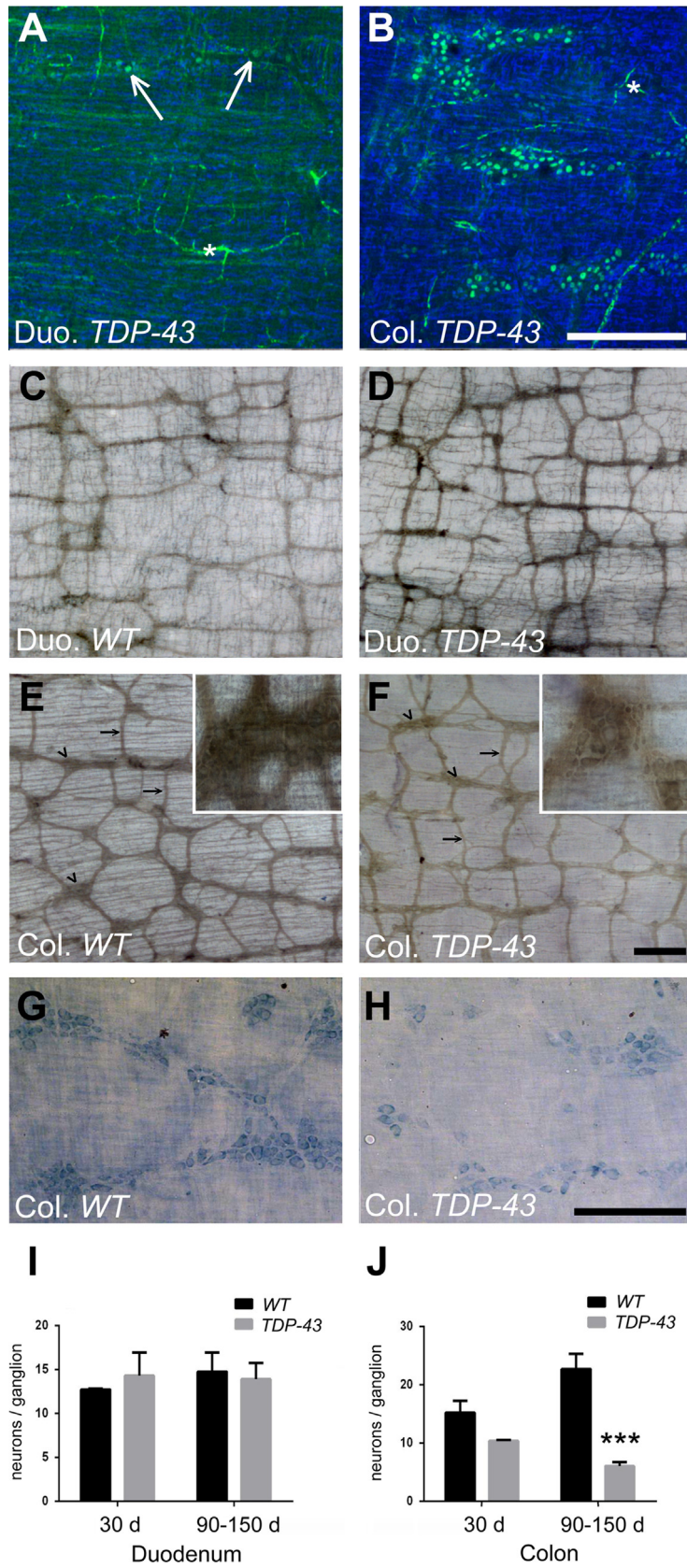


Fig. 3 – Expression of the TDP-43 transgene and neuropathy in the myenteric plexus. Anti-Flag immunofluorescence was used to detect the expression of the transgene in the *duodenum* (A) and *colon* (B) myenteric plexuses. Blood vessels were stained by the secondary antibody alone (asterisk). Acetylcholinesterase staining of the myenteric plexus of the *duodenum* (C, D) and *colon* (E, F) of 120 days old WT (C, E) and TDP-43 (D, F) mice. Insets in (E, F) show higher magnification pictures of the ganglions. Ganglions are showed by arrow heads and intermodal strands by arrows. Cuprolinic blue staining of the ganglion neurons in the myenteric plexus of TDP-43 (H) and WT mice (G). Scale bar corresponds to 250 μ m (insets are 50 μ m wide). Quantification of the number of neurons per ganglion in the myenteric plexus of the *duodenum* (I) and *colon* (J) in WT and TDP-43 mice ($n=3$ mice per genotype).

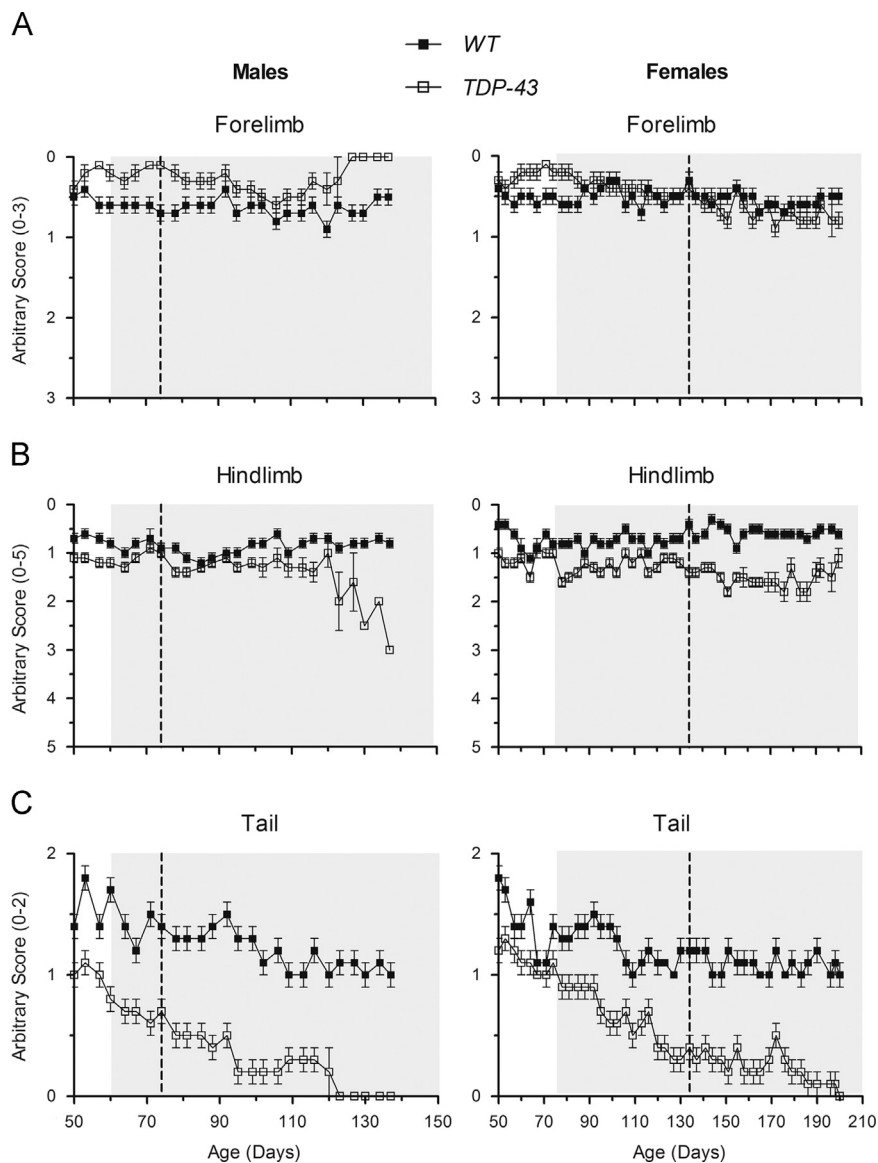


Fig. 4 – Phenotypic characterization. Forelimb (A) and hindlimb (B) reflexes were assessed when the mice were held by the base of their tail. Tail position (C) was assessed when the mice were moving. The gray areas represent measurements that took place after the onset of GI pathology. The dotted vertical lines represents the time of the first mouse death in the respective cohort. Details on scoring methods are in the Experimental Procedures section. $n = 60$ male TDP-43, 29 male WT, 56 female TDP-43, 30 female WT. Values represent the mean \pm SEM.

tails when walking (score 0), whereas their WT littermates held their tails slightly elevated (score 2) or parallel to the ground (score 1). The difference in tail elevation was already significant on the first day of testing (day 50), and it worsened progressively. Tail elevation impairments have previously been observed in the SOD1G93A mice as early as post-natal day 40, and they were described as the earliest neurological symptom in this mouse model (Alves et al., 2011). In TDP-43 mice the tail elevation impairment was present prior to the onset of GI pathology and perhaps represents an early clinical sign of disease.

The muscular strength of TDP-43 and WT mice was evaluated over time by means of the grip strength and the hanging wire tests. Both tests were performed on the same cohort of animals at post-natal age days 60, 75 and 90 for males and post-natal age days 60, 75, 90, 120 and 150 for females.

The grip strength test measured the maximum force generated by the forelimb or hindlimb muscles at a given instance. Male mice showed no overall differences in the force exerted by the forelimb and hindlimb muscles of TDP-43 and WT littermates at any time point tested (Fig. 5A and B, left panels). In female mice, the grip strength performance of WT mice improved with age, while TDP-43 mice retained similar muscle strength throughout the duration of the experiment. TDP-43 mice were able to exert a slightly greater force compared to WT littermates with their forelimb muscles, whereas WT mice were to exert a slightly greater force compared to TDP-43 mice with their hindlimb muscles (Fig. 5A and B, right panels). There were no grip strength differences between male and female TDP-43 mice.

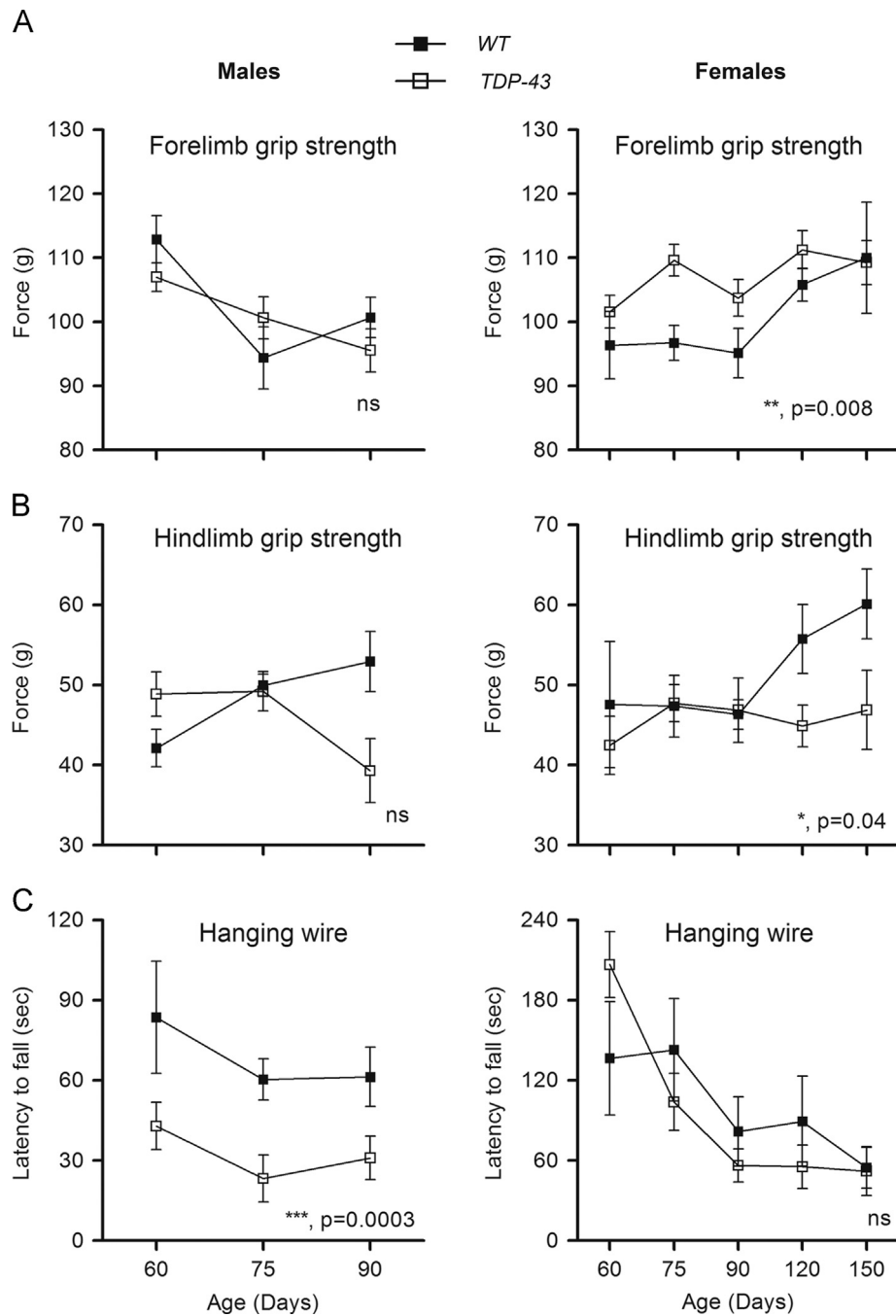


Fig. 5 – Muscular strength. Muscle strength was assessed using two different methods. By measuring the maximum force exerted by forelimbs (A) and hindlimbs (B) using a grip strength apparatus and by measuring the time in seconds that a mouse could support its own weight when hanging from a cage top wire (C). For the forelimb grip strength test $n=37$ male TDP-43, $n=22$ male WT, $n=34$ female TDP-43, and $n=18$ female WT. For the hindlimb grip strength test $n=18$ male TDP-43, $n=13$ male WT, $n=15$ female TDP-43, and $n=8$ female WT. For the hanging wire test $n=21$ male TDP-43, $n=9$ male WT, $n=20$ female TDP-43, and $n=9$ female WT. Values represent the mean \pm SEM.

The hanging wire test measured the ability of mice to produce sustained tension in the limb musculature to oppose the gravitational effect of their body weight. It measured the time it took for a mouse to fall off the metal grid. The results showed significant deficits in male TDP-43 mice compared with WT littermates at all times tested. At post-natal age 60, the “time to fall” for TDP-43 mice was 43 ± 9 s and for WT mice it was 84 ± 21 s. This two-fold difference in the “time to

fall” was conserved throughout the experiment. In contrast, there were no differences between female TDP-43 and WT littermates, even though the performance of both cohorts declined with age. The nature of this test does not permit attributing changes to specific neuromuscular deficits, but only to a generalized weakness with potentially varying causes, including exhaustion caused by GI or upper motor neuron pathology. There were significant gender differences

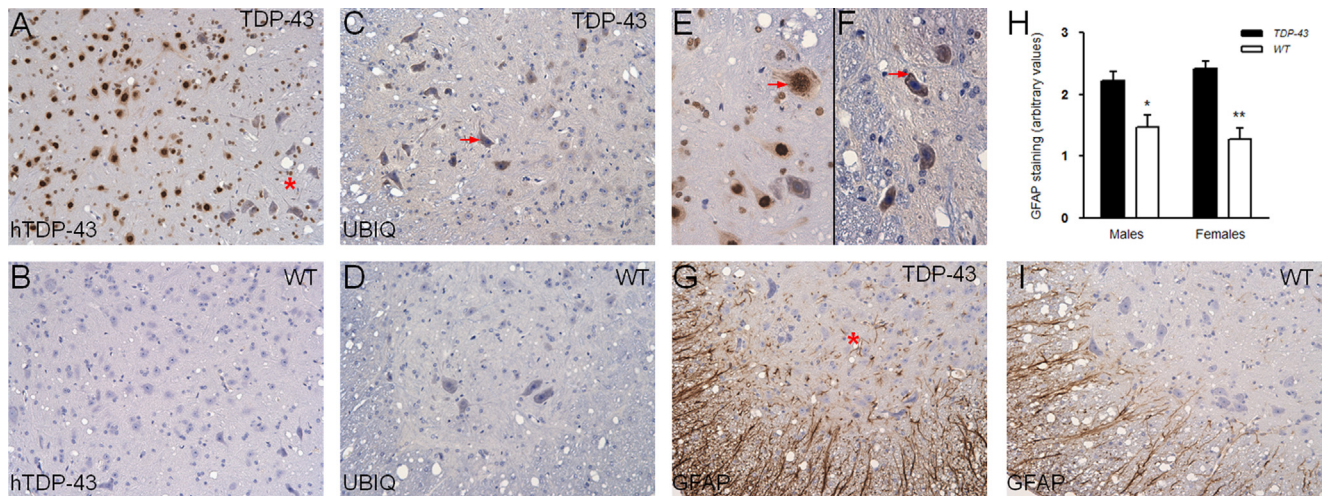


Fig. 6 – hTDP-43, ubiquitin and GFAP immunohistochemistry. Representative pictures (20 ×) showing immunohistochemistry on spinal cord lumbar sections with an antibody against human TDP-43 from 80-day old TDP-43 and WT male mice (A, C). The asterisk in A represents lamina IX, a region with reduced TDP-43 staining. Representative pictures (20 ×) showing immunohistochemistry with an anti-ubiquitin antibody on spinal cord lumbar sections from 80-day old TDP-43 and WT male mice (C, D). The arrow in (C) shows a motor neuron positive for ubiquitin. High magnification pictures (40 ×) showing an abnormally shaped TDP-43 positive nucleus noted with an arrow (E), and ubiquitin-positive cytoplasmic inclusions noted with an arrow (F). Quantification of GFAP staining in male and female TDP-43 and WT mice (H). Values represent the mean ± SEM. Representative pictures (20 ×) showing immunohistochemistry with an anti-GFAP antibody on spinal cord lumbar sections from 80-day old TDP-43 and WT male mice (G, I).

in hanging wire test results, with males falling off the metal grid much faster than the females. These differences were observed in both TDP-43 and WT cohorts and were presumed to be the consequence of the greater body weight of the male mice.

2.5. TDP-43, ubiquitin and GFAP immunostaining in the spinal cord

Immunostaining with a specific anti-human TDP-43 antibody revealed a strong and widespread expression of the exogenous transgene in the nuclei of sensory and motor neurons from the lumbar section of the spinal cord (Fig. 6A). Interestingly, in the region of lamina IX (Fig. 6A, asterisk) there was a subpopulation of large hindlimb-projecting MNs (The Christopher and Dana Reeve Foundation Spinal Cord Atlas, 2008), with reduced TDP-43 staining. This subpopulation of unstained MNs was present in all TDP-43 mice analyzed ($n=23$), independent of gender or age. There was no positive TDP-43 staining in the spinal cords of WT mice indicating that the anti-human TDP-43 antibody used did not cross-react with endogenous mouse TDP-43 protein (Fig. 6B).

Consecutive spinal cord sections from the same mice were stained with a polyclonal anti-ubiquitin antibody. Results showed increased ubiquitin-positive staining in the spinal cord sections of TDP-43 mice compared to WT controls (Fig. 6C and D). Unlike TDP-43 staining, ubiquitin staining was restricted to the cytoplasm of large MNs in the ventral horn of the SC (Fig. 6C, arrow) and was absent from sensory neurons or glia.

A major histological hallmark of ALS is the presence of cytoplasmic inclusions positive for both ubiquitin and TDP-43 in the large MNs of the ventral horn of the SC. For this

reason the spinal cord cross-sections of all animals were carefully examined for the presence of these features. There was no clear evidence of mislocalized cytoplasmic TDP-43 or TDP-43-positive aggregates in any of the sections examined. Nevertheless, abnormally shaped TDP-43-positive nuclei were present in the large MNs of some animals (Fig. 6E, arrows), which may be a manifestation of cellular stress. In addition, there were several MNs with punctate ubiquitin staining, indicative of small aggregates (Fig. 6F, arrow).

Immunostaining for the glial fibrillary acidic protein (GFAP), a marker of differentiated astrocytes, revealed increased staining in the lumbar spinal cords of TDP-43 mice compared to WT littermates (Fig. 6G and I). Semiquantitative analysis revealed that the amount of GFAP immunostaining in the SC was 151% of WT controls in male TDP-43 mice. In female TDP-43 mice GFAP staining was 189% of WT controls (Fig. 6H). The increased GFAP staining was present in both the white and gray matter of TDP-43 mice, where the axonal tracks and cell bodies are respectively located. Furthermore, only TDP-43 mice showed reactive astrogliosis in the region normally occupied by large motor neuron cell bodies (Fig. 6G, asterisk).

In small groups of male mice, femoral nerves were harvested at three and five months of age (Supplemental Materials; Fig. S4). Examining these revealed that the number and diameter of axons in the motor branch of the femoral nerve of TDP-43 mice were not significantly different from WT controls (Fig. S4C and D), despite a 20% reduction in neuromuscular junction postsynaptic area (Fig. S5C). Thus, muscles of TDP-43 mice appear to be normally innervated through five months of age. Interestingly, there was a small but significant decrease in axon number and diameter in the sensory branch of the femoral nerve in both the 3- and 5-month old TDP-43 mice (Fig. S4E and F).

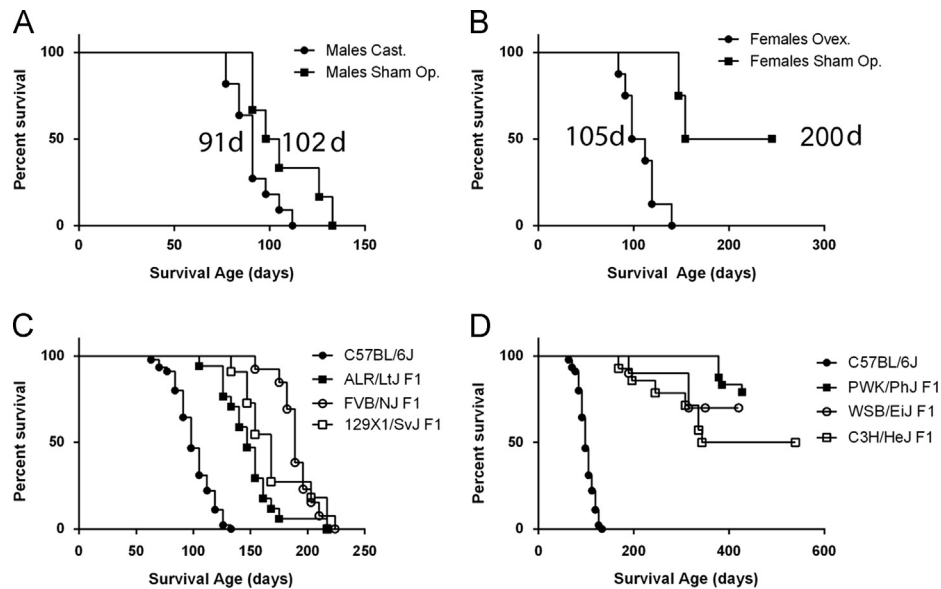


Fig. 7 – Gender and genetic background affect the survival of TDP-43 transgenic mice. Kaplan–Meier curve showing the survival of castrated ($n=11$) or sham-operated ($n=6$) TDP-43 males (A). Castrations mildly reduced survival (Log-rank Mantel-Cox test $p=0.047$, median survival of 91 and 102 days respectively). Kaplan–Meier curve showing the survival of ovariectomized ($n=8$) or sham-operated ($n=4$) TDP-43 females (B). Ovariectomies strongly reduced survival (Log-rank Mantel-Cox test $p=0.0025$, median survival of 105 and 200 days respectively). Kaplan–Meier curve showing the survival of “short-lived” F1 transgenic mice compared to C57BL6/J transgenic mice (C; C57BL6/J: $n=45$, ALR/LtJ: $n=15$, FVB/NJ: $n=13$, 129 × 1/SvJ: $n=11$). Kaplan–Meier curve showing the survival of “long-lived” F1 transgenics compared to C57BL6/J transgenic mice (D; C57BL6/J: $n=45$, PWK/PhJ: $n=13$, WSB/EiJ: $n=10$, C3H/HeJ: $n=14$). All F1 mice displayed statistically significant differences in survival compared to C57BL6/J TDP-43 transgenic mice.

2.6. Gender differences and genetic background contributions

The current study identified significant gender differences in the onset and severity of GI pathology and consequently in the survival of male and female TDP-43 mice. To determine whether these gender effects were related to differential expression of the hTDP-43 transgene, qPCR measurements of transgene expression were performed on GI tract samples from male and female TDP-43 mice. Results showed that both genders expressed the transgene at equal levels (data not shown).

To explore gonadal hormone contributions to gender differences in disease manifestation, survival duration of orchietomized male or ovariectomized female mice was compared to that of age- and gender-matched sham-operated TDP-43 mice (Fig. 7A and B). Male castration had a small effect on median survival, decreasing it by 10 days (Fig. 7A). Female ovariectomy had a major effect on median survival decreasing it by about 94 days (Fig. 7B), bringing it closer to the typical median survival for male TDP-43 mice. The effect of ovariectomy on the onset or severity of GI pathology was not investigated. Nevertheless, these data suggest that estrogen may play a protective role in the less-aggressive disease course shown in female TDP-43 mice.

It is important to note that the transgenic line was originally developed and characterized in a non-congenic C57BL/6J genetic background and as described in the initial publication, the mice showed a phenotype that was markedly different from the one described herein. Specifically, no gut

pathology was described and considerable neuro-muscular deficits were identified, (Wegorzewska et al., 2009). Subsequent to the original publication describing these mice, a backcross to C57BL/6J was initiated. The mice were backcrossed five generations then sent to the Jackson Laboratory, where the backcross was completed (see Section 4). Prior to our knowledge of a gastrointestinal phenotype, we began to investigate the effects of genetic background on the phenotype of TDP-43 mice, by conducting a screen for dominant genetic modifiers. Prp-TDP43A315T mice on a congenic C57BL/6 background were crossed with mice of different genetic backgrounds (ALR/LtJ, FVB/NJ, 129S1/SvImJ, PWK/PhJ, WSB/EiJ, and C3H/HeJ) and the phenotypes of hemizygous TDP-43 male progeny (F1) were compared. All the F1's had an extended survival compared to male TDP-43 mice on a congenic C57BL/6 genetic background (Fig. 7C and D). Survival was increased by 50–90 days in males of the ALR/LtJ, FVB/NJ and 129S1/SvJ F1's (Fig. 7C), and by more than 340 days for males of the C3H/HeJ, WSB/EiJ and PWK/PhJ F1's (Fig. 7D). Even though the genetic background significantly affected the median survival of male TDP-43 mice, it did not appear to affect the phenotype or the cause of death of these mice. Similarly to their TDP-43 counterparts on a congenic C57BL/6 background, all F1's died with visible signs of gut pathology. F1 animals did not show any gross neuromuscular deficits by visual examination however histological examination of the femoral nerves of a small number of each F1 progeny revealed differences between genetic backgrounds that remain to be fully characterized (data not shown).

3. Discussion

Historically, the field of ALS therapy development has been hampered by a shortage of good genetic animal models. The quest for useful genetic models has in part been affected by the fact that only 10% of ALS cases are inherited, with approximately half of these familial cases currently attributable to specific gene mutations. Recent advances in sequencing have made the identification of new and rare genetic mutations of ALS possible, such as mutations in the TDP-43 gene. As a result, numerous mouse models with ALS-associated mutations are being created. While mouse models are often useful for elucidating disease mechanisms and in preclinical trials of potential therapeutics, they occasionally exhibit co-morbidity phenotypes that are not reflective of the primary human deficit. The objective of this research was to determine whether the phenotype of the C57BL/6J congenic Prp-TDP43A315T mouse model is consistent with the phenotype of ALS and therefore whether it is an appropriate model for testing therapeutics specifically developed for humans with ALS.

Our findings show that the current Prp-TDP43A315T mouse model does not recapitulate many of the key features of ALS. Any motor deficits or muscle weakness in these mice are mild. There are no detected gait abnormalities, no signs of paralysis, and no obvious cytoplasmic TDP-43 aggregates. Moreover, the decreased life-span of these mice does not appear to be caused by MN abnormalities as reported in the original colony. Instead, the decreased survival appears to be related to neurodegeneration in the myenteric plexus of the colon as others have also reported (Guo et al., 2012). While there have been studies noting increased constipation in ALS patients (Mannino et al., 2007), to our knowledge there are no case studies suggesting that a similar type of neurodegeneration is present in ALS patients. Thus, the neurodegeneration in the lower GI tract appears to be a unique feature of the Prp-TDP43A315T mouse model that is likely caused by the site-specific overexpression of the transgene in the lower GI. In the upper GI, where the transgene is not expressed to the same degree, there was no evidence of neurodegeneration.

The Prp-TDP43A315T mice studied in this research show a phenotype that is distinctly different from the one described in previous reports. These differences in phenotype can be to some extent explained by differences in the genetic background of the original published line (mixed C57BL6/CBA genetic background) and the line as it exists today (fully congenic C57BL/6J). Genetic heterogeneity accounts for a great deal of phenotypic variability in both humans and mice. Mice on a mixed genetic segregating background often create problems in reproducibility of data across laboratories, as many alleles that can contribute to resistance or susceptibility to a particular trait can be fixed or selected against as a result of continuous breeding. To guard against this, the standardization of alleles on a congenic genetic background is a common practice, and was applied to this model. A dominant modifier screen against the fully congenic Prp-TDP43A315T mice is reported herein, supporting the hypothesis that the phenotype of this line is very susceptible to changes in genetic background. This is illustrated by the fact

that all of the offspring derived from this screen have significantly extended life-spans compared to the life-spans of fully congenic Prp-TDP43A315T mice. While the C57BL6/J line was not specifically crossed to the CBA line to test for restoration of the initial phenotype, it was crossed to C3H, a line that closely resembles CBA (Atchley and Fitch, 1993; Whitmore and Whitmore, 1985). The C57BL6/C3H F1 generation demonstrated extended survival relative to the C57BL6/J congenic strain but still did not reveal an ultimate end-stage phenotype markedly different from that of the C57BL6/J congenic strain. A more extensive study searching for genetic modifiers of the Prp-TDP43A315T transgenic phenotypes could reveal phenotypes suggestive of lower motor neuron pathology and could lead to the discovery of genes relevant to the study of ALS. However, it was beyond the scope of this report.

Gender differences may also be partly responsible for the differences in the phenotype observed in this research and previous studies. The original publication on the Prp-TDP43A315T model indicated that the mean survival was 153 days, however the data were not stratified based on gender. Our data indicate clear gender differences in Prp-TDP43A315T mice with respect to disease onset, severity, progression and their subsequent survival despite similar levels of transgene expression. Male TDP-43 animals have a more consistent rapid onset of disease with a median survival of 108 days, whereas female TDP-43 animals live considerably longer and have a median survival of 185 days. Moreover, ovariectomizing females results in a survival curve that is very similar to that of male mice, suggesting a protective role for estrogen. Conversely, castration of males does not have a major effect on survival. While the mechanism of “estrogen protection” with respect to neurodegeneration is beyond the scope of this paper, it is worth noting that improved performance in females relative to males is a common theme in other rodent ALS models, for example in the high copy SOD1G93A mouse model. Further, human clinical epidemiology studies demonstrate a higher incidence of ALS in males compared to females (McCombe and Henderson, 2010). Exploration of the mechanisms underlying the less severe disease phenotype in females, in the TDP-43 and other mouse models, might provide insight into potential therapeutic pathways.

Even though both genetic background and gender impact many aspects of the phenotype of Prp-TDP43A315T mice, these factors do not seem to alter the cause of death. In all cases, the death of the animals, whether early or delayed, coincided with a severe GI pathology. This indicates that denervation of the colon remained the principle contributor to morbidity. In no case was there an obvious ALS-like phenotype. It has been suggested that prion-promoter-driven overexpression of mutant hTDP-43 would have eventually caused an ALS-like phenotype if the mice had not first succumbed to complications relating to the denervation of the colon (Esmaeili et al., 2013). However, both female TDP-43 mice and male offspring from the genetic background screen lived significantly longer than male TDP-43 mice, without developing an ALS-like phenotype. This suggests that the neuromuscular system in the current Prp-TDP43A315T congenic strains is not very sensitive to transgene expression. Nevertheless, gut motility deficits that directly correlate with

the progressive neurodegeneration in the colon could cause performance deficits in phenotypic tests like the hanging wire, or the “swimming gait” as described by others (Esmaeili et al., 2013), thereby complicating the interpretation of standalone neuromotor assessments.

Histological experiments performed in this research indicate that Prp-TDP43A315T mice do exhibit some pathological signs of ALS even though they lacked key phenotypic features of the disease. Ubiquitinated inclusions, present in spinal cord MNs of humans with ALS, were also present in these mice. The pattern of GFAP staining in the white matter of the spinal cord of Prp-TDP43A315T mice may also reflect some axonal tract degeneration. In contrast, TDP-43 cytoplasmic aggregates, nearly ubiquitous in post mortem spinal cord samples from humans with ALS, were completely absent in spinal cord MNs from these mice despite, robust staining of human TDP-43 in the MN nuclei. Further, there was no evidence of axonal loss in the motor branch of the femoral nerve. The brain of these mice was not examined and therefore it is not known how the brain pathology of Prp-TDP43A315T mice relates to frontotemporal dementia or whether there may be signs of pathology in the upper MNs of these mice.

The comprehensive evaluation of the Prp-TDP43A315T mice undertaken in this study in many ways illustrates the complexity and difficulty of designing, generating, and characterizing a genetically engineered mouse model of human ALS disease. The current work directly highlights contributions of genetic background, gender, tissue and cell specific sensitivities to mutant transgene expression, and variable expression levels within similar cell types. All are important factors that can influence the stability and viability of a transgenic rodent ALS model. In conclusion, while the Prp-TDP43A315T model may be useful for studying GI tract neurodegeneration, it does not display a phenotype suitable for testing ALS therapeutics. Future experiments involve the examination of other existing TDP-43 generated transgenic models to ascertain whether neurodegeneration in the myenteric plexus is also present in these models and if genetic background and prion promoter driven expression correlate with this phenotype.

4. Experimental procedures

4.1. Animal breeding, care and experimentation

Transgenic mice with the A315T human TDP-43 mutation under the control of the mouse prion promoter and an N-terminal Flag tag were originally developed by Dr. Robert Baloh (Washington University School of Medicine, St. Louis, MO). These transgenic mice were backcrossed for approximately five generations into a C57BL/6J background when they were donated to The Jackson Laboratory (Bar Harbor, ME). The colony studied at ALS TDI was expanded and maintained at Charles River where all the genotyping was performed (Wilmington, MA). Male mice were singly housed and female mice were housed four per cage except in cohorts used to evaluate food intake and gut motility. In these studies all mice were singly housed.

At The Jackson Laboratory (stock number 010700), mice were received after having been crossed five times to C57BL6/J. They were crossed to C57BL6/J for three more generations with marker-assisted selection (“speed congenics” approach). Briefly, transgenic mice at each generation were genotyped with a 122 SNP panel (The Jackson Laboratory, KBioscience) to select breeders for the next generation with the most C57BL6/J haplotypes. Mice homozygous for the C57BL6/J haplotypes at the 122 SNPs tested were used to establish the pure congenic production colony. Animals were housed at a density not exceeding five adult mice per hemi-cage, under specific pathogen free conditions.

Mice were housed in rooms with a 12 h light/12 h dark cycle at temperature of 18–23 °C and 40–60% humidity. Food and water were provided ad libitum. The diet used was Teklad Global diet #2918 for rodents (Harlan Laboratories, Houston, TX). All mice in this study were observed daily for signs of distress. With the exception of the genetic background experiment, all the mice used in this study were on a congenic C57BL/6J background. All experiments were conducted in accordance with the protocols described by the National Institutes of Health Guide for the Care and Use of Animals and were approved by The Jackson Laboratory's (JAX) and ALS TDI's respective institutional animal care and use committees.

4.2. Whole gut motility assay

Intestinal transit time was assessed using a whole gut motility assay which was previously described (Nagakura et al., 1996). Briefly, 0.3 ml of a non-toxic 5% solution of indigo (blue) carmine dye (Sigma, St. Louis, MI) dissolved in 0.5% methylcellulose, was administered to mice via oral gavage and the mice were then returned to their individual cages. Cages were visually inspected hourly for 12 h for the presence of blue fecal pellets. The intestinal transit time for each mouse was taken as the hours required from the administration of the blue carmine dye to the first appearance of a blue pellet. Cages without a blue fecal pellet after 12 h were re-inspected at 24 h. At that time, if a blue pellet was present the endpoint was recorded as 13 h. If no blue pellet was present the endpoint was recorded as 24 h.

4.3. Phenotypic characterization

Four different cohorts of mice were evaluated twice a week using a modified version of the SHIRPA protocol (Rogers et al., 1997) that concentrated on identifying neurological abnormalities. Each cohort was managed by a different experimenter and the results were combined for the final analysis. Each mouse was observed in three different settings for a total time of about 1 min each: in a viewing jar, in an open-field arena and when held by the tail. The following observations were made: body weight, body position, hair-coat appearance, trunk curl, tremor, hindlimb clasping, tail position, forelimb reflexes, and hindlimb reflexes. Each observation was scored on an arbitrary scale. To assess tail position the mouse was observed in motion. Scoring was as follows: 0=tail dragging; 1=tail parallel to the ground; and 2=tail elevated. To assess forelimb reflex the mouse was held by the tail and lifted vertically. Scoring was as follows:

0=forelimbs reached forward; 1=forelimbs were retracted; and 2=forelimbs retracted and pushed against body. To assess hindlimb reflex the mouse was also held by the tail and lifted vertically. Scoring was as follows: 0=full extension away from midline; 1=full extension with trembling/shaking; 2=collapse or partial collapse; 3=hindlimbs folded back/pushed against body; 4=hindlimbs beginning to paralyze, dragged when in motion; and 5=rigid paralysis, no movement. Left and right forelimbs and hindlimbs were scored separately and the average score was calculated. All moribund mice were excluded from this analysis.

4.4. Muscular strength

The muscular strength of the same cohort of mice was assessed using two different tests: the grip strength and the hanging wire tests. The forelimb and hindlimb grip strength test was performed using a commercially available apparatus (BioSeb, Chaville, France). Each mouse was held by the tail and was allowed to grasp a metal grid attached to a force meter using its forelimbs. The mouse was then pulled horizontally and steadily away from the meter following the axis of the grid. The maximum grasping force of the mouse was recorded on the force meter. For testing the hindlimbs the same general procedure was followed, but in this case the mouse was gently restrained behind the neck and was held at an angle so that only the hindlimbs touched the metal grid. The average of three measurements per time point per mouse was used for the analysis. For the hanging wire test, mice were placed on the top of a standard wire cage lid. The lid was gently shaken to allow animals to grip firmly, then turned upside down and placed at about 30–40 cm high above the cage litter. The latency to fall off the wire lid was measured using a stop-watch with a 300 s cut-off period. Mice were excluded from these tests if they were considered to be sick. Body weights have an impact on how the animals perform in these tests, however in this study at the start of the experiment, the average body weights of TDP-43 and wild-type animals were not significantly different and thus the values were left unadjusted for weight.

4.5. Myenteric plexus immunohistochemistry

Mice were euthanized, and their intestines were dissected out and fixed overnight in 2% paraformaldehyde (PFA) in phosphate buffer (PBS). The myenteric plexus was prepared as previously described (Osorio and Delmas, 2010). Briefly, 1cm long sections of the digestive tube were incised longitudinally following the junction with the mesentery and pinned down open on a silicone dish, in PBS, with the mucosa facing up. The mucosa was peeled away and the underlying muscle layers transferred and spread on microscope slides and let to air dry. Adhering intestinal wall flat mounts were then processed for staining as described below. (1) Anti-flag immunofluorescence was performed on flat mounts using the following antibodies and reagents: mouse monoclonal ANTI-FLAG[®] M2 (Sigma, St. Louis, MO) and Alexa Fluor[®] 488 Goat Anti-Mouse IgG (Life Technologies, Beverly, MA). (2) Cuproline blue staining of the myenteric plexus neurons was performed as previously described (Holst and Powley, 1995). Briefly, a solution of quinolinic phthalocyanine

(Polysciences, Warrington, PA) at 0.5% (w/v) in 0.05 M sodium acetate buffer, pH 5.6, 1 M MgCl₂ was applied on the slides. After 1 h of incubation at 37 °C, preparations were differentiated for 2 min in 0.05 M sodium acetate buffer, pH 5.6 with 1 M MgCl₂, air dried, and mounted in Permount (Fisher Scientific, Waltham, MA). (3) Acetylcholinesterase staining was performed on intestine flat mounts by incubating them for 1 h in saturated sodium sulfate solution in water, and then transferring them to the staining solution (0.2 mM ethopropazine hydrochloride, 4 mM acetylthiocholine iodide, 10 mM glycine, 3 mM cupric sulfate and 100 mM sodium acetate, adjusted to pH 5.5 with glacial acetic acid) for 2 h. Preparations were washed five times in water, placed for about 1 min in a 1.25% solution of sodium sulfide in water (adjusted to pH 6 with hydrochloric acid), rinsed again in water, air dried and mounted in Permount (Fisher Scientific, Waltham, MA).

4.6. Spinal cord immunohistochemistry

Mice of different genotypes, genders and ages were anesthetized and transcardially perfused with 4% PFA in PBS. The vertebral columns containing the intact spinal cords were extracted and further fixed in the same fixative for at least 24 h before being transferred to a 70% ethanol solution for storage. Prior to processing, the vertebral columns were decalcified in formic acid and then embedded into paraffin blocks. The tissues were sectioned at 5 mm and mounted on SuperFrost glass slides. Classical histochemistry was performed according to standard protocols. Sections were deparaffinized and rehydrated, pretreated with warm citrate buffer for 20 min to enhance immunoreactivity, incubated with 3% H₂O₂ for 12 min at room temperature to quench endogenous peroxidases, and blocked with 2% horse serum for 20 min at room temperature. Sections were incubated overnight at 4 °C with a mouse monoclonal anti-human TARDBP (1:1000; Santa Cruz Biotechnology, CA) or a rabbit polyclonal anti-ubiquitin (1:200; Abcam, Cambridge, MA) or a mouse monoclonal anti-GFAP (1:1000; Abcam, Cambridge, MA) primary antibody. The next day, sections were incubated for 1 h at room temperature in a biotinylated goat anti-mouse IgG secondary antibody and processed with the avidin–biotin complex (ABC; Vector Laboratories). Immunolabeling was revealed after incubation in a DAB/Metal Concentrate for 1 min and sections were counterstained with Harris hematoxylin. Sections were dehydrated and cover-slipped. Photomicrographs were taken by light microscopy using a MBF CX9000 digital camera (MBF Bioscience) connected to an Olympus BX51 microscope, with 4×, 20× and 40× objectives, and controlled by the Stereo Investigator software (MBF Bioscience). Semi-quantitative analysis of GFAP immunostaining was performed on lumbar spinal cord sections taken with the 4× objective by three different observers blind to the experimental groups on an arbitrary scale (1=none or little staining; 2=some staining; and 3=abundant staining). The value used for analysis was the average value of the three observers.

4.7. Orchiectomies and ovariectomies

Mice undergoing surgery were anesthetized with tribromoethanol (400 mg/kg, intraperitoneal) and were administered

carprofen, as an analgesic, before they awoke from the anesthesia. For orchiectomies (castrations), the ventral skin and abdominal wall of male mice were incised, the tail of the epididymis was sectioned and testicular artery cauterized, before testicles were excised. For ovariectomies, the lateral skin and abdominal wall of female mice were incised, the uterine horn was sectioned and its blood vessels cauterized and the ovaries removed. Incisions were sutured and mice were observed daily after the surgery to ensure that they healed properly. All surgeries were performed by the surgical services staff of The Jackson Laboratory, following IACUC approved procedures. Veterinarians were consulted if necessary during the recovery period.

4.8. Statistical analyses

Kaplan–Meier survival analysis was used for survival comparisons. The Student's *t*-test was used for GFAP immunostaining and myenteric and ganglionic neuron counts. The chi-squared test was used for categorical data analysis in the phenotypic characterization experiment. A two-way ANOVA (with repeated measures where applicable) was used in all other cases. Statistical significance was determined based on the following *p* values as follows: **p* < 0.05, ***p* < 0.01, ****p* < 0.005, and *****p* < 0.0001. In cases where there was an overall statistical significance, post-hoc tests were performed using Bonferroni's method. Data were presented as mean ± SEM. All data were analyzed using GraphPad Prism version 5.00 for Windows (GraphPad Software, Inc., San Diego, CA).

Acknowledgments

We thank Dr. Ian Mackenzie for advice on the immunohistochemistry experiments, Drs. Michelle Pflumm and Alan Gill for editing the manuscript, Ricky Sanchez for technical assistance and our funding agencies: Alzheimer's Drug Discovery Foundation, The Association for Frontotemporal Degeneration, and Muscular Dystrophy Association. We also wish to thank the ALS Association, The Tow Foundation, and ALS Therapy Alliance for supporting the ALS mouse Repository at The Jackson Laboratory, Racheal Wallace for her technical assistance and Chuck Dangler for his expertise in intestinal pathology.

Appendix A. Supporting information

Supplementary data associated with this article can be found in the online version at <http://dx.doi.org/10.1016/j.brainres.2013.10.013>.

REFERENCES

- Aggarwal, S., Cudkovic, M., 2008. ALS drug development: reflections from the past and a way forward. *Neurotherapeutics* 5, 516–527.
- Alves, C.J., de Santana, L.P., dos Santos, A.J., de Oliveira, G.P., Duobles, T., Scorisa, J.M., Martins, R.S., Maximino, J.R., Chadi,

- G., 2011. Early motor and electrophysiological changes in transgenic mouse model of amyotrophic lateral sclerosis and gender differences on clinical outcome. *Brain Res.* 1394, 90–104.
- Arai, T., Hasegawa, M., Akiyama, H., Ikeda, K., Nonaka, T., Mori, H., Mann, D., Tsuchiya, K., Yoshida, M., Hashizume, Y., Oda, T., 2006. TDP-43 is a component of ubiquitin-positive tau-negative inclusions in frontotemporal lobar degeneration and amyotrophic lateral sclerosis. *Biochem. Biophys. Res. Commun.* 351, 602–611.
- Atchley, W.R., Fitch, W., 1993. Genetic affinities of inbred mouse strains of uncertain origin. *Mol. Biol. Evol.* 10, 1150–1169.
- Barbeito, L.H., Pehar, M., Cassina, P., Vargas, M.R., Peluffo, H., Viera, L., Estevez, A.G., Beckman, J.S., 2004. A role for astrocytes in motor neuron loss in amyotrophic lateral sclerosis. *Brain Res. Rev.* 47, 263–274.
- Benatar, M., 2007. Lost in translation: treatment trials in the SOD1 mouse and in human ALS. *Neurobiol. Dis.* 26, 1–13.
- Esmaeili, M.A., Panahi, M., Yadav, S., Hennings, L., Kiaei, M., 2013. Premature death of TDP-43 (A315T) transgenic mice due to gastrointestinal complications prior to development of full neurological symptoms of amyotrophic lateral sclerosis. *Int. J. Exp. Pathol.* 94, 56–64.
- Ghatak, N.R., Campbell, W.W., Lippman, R.H., Hadfield, M.G., 1986. Anterior horn changes of motor neuron disease associated with demyelinating radiculopathy. *J. Neuropathol. Exp. Neurol.* 45, 385–395.
- Gitcho, M.A., Baloh, R.H., Chakraverty, S., Mayo, K., Norton, J.B., Levitch, D., Hatanpaa, K.J., White III, C.L., Bigio, E.H., Caselli, R., Baker, M., Al-Lozi, M.T., Morris, J.C., Pestronk, A., Rademakers, R., Goate, A.M., Cairns, N.J., 2008. TDP-43 A315T mutation in familial motor neuron disease. *Ann. Neurol.* 63, 535–538.
- Gordon, P.H., Meininger, V., 2011. How can we improve clinical trials in amyotrophic lateral sclerosis? *Nat. Rev. Neurol.* 7, 650–654.
- Guo, Y., Wang, Q., Zhang, K., An, T., Shi, P., Li, Z., Duan, W., Li, C., 2012. HO-1 induction in motor cortex and intestinal dysfunction in TDP-43 A315T transgenic mice. *Brain Res.* 1460, 88–95.
- Gurney, M.E., Cutting, F.B., Zhai, P., Doble, A., Taylor, C.P., Andrus, P.K., Hall, E.D., 1996. Benefit of vitamin E, riluzole, and gabapentin in a transgenic model of familial amyotrophic lateral sclerosis. *Ann. Neurol.* 39, 147–157.
- Gurney, M.E., Pu, H., Chiu, A.Y., Dal Canto, M.C., Polchow, C.Y., Alexander, D.D., Caliendo, J., Hentati, A., Kwon, Y.W., Deng, H.X., 1994. Motor neuron degeneration in mice that express a human Cu,Zn superoxide dismutase mutation. *Science* 264, 1772–1775.
- Holst, M.C., Powley, T.L., 1995. Cuproinic blue (quinolinic phthalocyanine) counterstaining of enteric neurons for peroxidase immunocytochemistry. *J. Neurosci. Methods* 62, 121–127.
- Knowles, C.H., Martin, J.E., 2000. Slow transit constipation: a model of human gut dysmotility. Review of possible aetiologies. *Neurogastroenterol. Motil.* 12, 181–196.
- Leigh, P.N., Whitwell, H., Garofalo, O., Buller, J., Swash, M., Martin, J.E., Gallo, J.M., Weller, R.O., Anderton, B.H., 1991. Ubiquitin-immunoreactive intraneuronal inclusions in amyotrophic lateral sclerosis. Morphology, distribution, and specificity. *Brain* 114 (Pt. 2), 775–788.
- Ludolph, A.C., Bendotti, C., Blaugrund, E., Chio, A., Greensmith, L., Loeffler, J.P., Mead, R., Niessen, H.G., Petri, S., Pradat, P.F., Robberecht, W., Ruegg, M., Schwalenstocker, B., Stiller, D., van den, B.L., Vieira, F., von, H.S., 2010. Guidelines for preclinical animal research in ALS/MND: a consensus meeting. *Amyotroph. Lateral Scler.* 11, 38–45.
- Maifirino, L.B., Liberti, E.A., Watanabe, I., de Souza, R.R., 1999. Morphometry and acetylcholinesterase activity of the myenteric neurons of the mouse colon in the chronic phase

- of experimental *Trypanosoma cruzi* infection. *Am. J. Trop. Med. Hyg.* 60, 721–725.
- Mannino, M., Cellura, E., Grimaldi, G., Volanti, P., Piccoli, F., La Bella, V., 2007. Telephone follow-up for patients with amyotrophic lateral sclerosis. *Eur. J. Neurol.* 14, 79–84.
- Marieb, E., Hoehn, K., 2012. *Human Anatomy and Physiology*. Benjamin-Cummings Publishing Company, San Francisco, CA.
- McCombe, P.A., Henderson, R.D., 2010. Effects of gender in amyotrophic lateral sclerosis. *Gend. Med.* 7, 557–570.
- Murayama, S., Inoue, K., Kawakami, H., Bouldin, T.W., Suzuki, K., 1991. A unique pattern of astrocytosis in the primary motor area in amyotrophic lateral sclerosis. *Acta Neuropathol.* 82, 456–461.
- Nagakura, Y., Naitoh, Y., Kamato, T., Yamano, M., Miyata, K., 1996. Compounds possessing 5-HT₃ receptor antagonistic activity inhibit intestinal propulsion in mice. *Eur. J. Pharmacol.* 311, 67–72.
- Neumann, M., Sampathu, D.M., Kwong, L.K., Truax, A.C., Micsenyi, M.C., Chou, T.T., Bruce, J., Schuck, T., Grossman, M., Clark, C.M., McCluskey, L.F., Miller, B.L., Masliah, E., Mackenzie, I.R., Feldman, H., Feiden, W., Kretschmar, H.A., Trojanowski, J.Q., Lee, V.M., 2006. Ubiquitinated TDP-43 in frontotemporal lobar degeneration and amyotrophic lateral sclerosis. *Science* 314, 130–133.
- Osorio, N., Delmas, P., 2010. Patch clamp recording from enteric neurons in situ. *Nat. Protoc.* 6, 15–27.
- Rogers, D.C., Fisher, E.M., Brown, S.D., Peters, J., Hunter, A.J., Martin, J.E., 1997. Behavioral and functional analysis of mouse phenotype: SHIRPA, a proposed protocol for comprehensive phenotype assessment. *Mamm. Genome* 8, 711–713.
- Rosen, D.R., Siddique, T., Patterson, D., Figlewicz, D.A., Sapp, P., Hentati, A., Donaldson, D., Goto, J., O'Regan, J.P., Deng, H.X., 1993. Mutations in Cu/Zn superoxide dismutase gene are associated with familial amyotrophic lateral sclerosis. *Nature* 362, 59–62.
- Rowland, L.P., Shneider, N.A., 2001. Amyotrophic lateral sclerosis. *N. Engl. J. Med.* 344, 1688–1700.
- Schiffer, D., Cordera, S., Cavalla, P., Migheli, A., 1996. Reactive astrogliosis of the spinal cord in amyotrophic lateral sclerosis. *J. Neurol. Sci.* 139 (Suppl.), 27–33.
- Scott, S., Kranz, J.E., Cole, J., Lincecum, J.M., Thompson, K., Kelly, N., Bostrom, A., Theodoss, J., Al-Nakhala, B.M., Vieira, F.G., Ramasubbu, J., Heywood, J.A., 2008. Design, power, and interpretation of studies in the standard murine model of ALS. *Amyotroph. Lateral Scler.* 9, 4–15.
- Sreedharan, J., Blair, I.P., Tripathi, V.B., Hu, X., Vance, C., Rogelj, B., Ackerley, S., Durnall, J.C., Williams, K.L., Buratti, E., Baralle, F., de Belleruche, J., Mitchell, J.D., Leigh, P.N., Al-Chalabi, A., Miller, C.C., Nicholson, G., Shaw, C.E., 2008. TDP-43 mutations in familial and sporadic amyotrophic lateral sclerosis. *Science* 319, 1668–1672.
- Swarup, V., Julien, J.P., 2011. ALS pathogenesis: recent insights from genetics and mouse models. *Prog. Neuropsychopharmacol. Biol. Psychiatry* 35, 363–369.
- Van Ginneken, C.J., De Smet, M.J., Van Meir, F.J., Weyns, A.A., 1999. Microwave staining of enteric neurons using cuproinic blue (quinolinic phthalocyanine) combined with enzyme histochemistry and peroxidase immunohistochemistry. *J. Histochem. Cytochem.* 47, 13–22.
- Wegorzewska, I., Bell, S., Cairns, N.J., Miller, T.M., Baloh, R.H., 2009. TDP-43 mutant transgenic mice develop features of ALS and frontotemporal lobar degeneration. *Proc. Natl. Acad. Sci. USA* 106, 18809–18814.
- Whitmore, A.C., Whitmore, S.P., 1985. Subline divergence within L.C. Strong's C3H and CBA inbred mouse strains. A review. *Immunogenetics* 21, 407–428.